Figure 4. Expression pattern of surface cell markers on Dox-responsive hADMPCs. Dox-responsive hADMPCs after selection by blasticidin were cultured in the absence (Dox(-)) or presence (Dox (+)) of 1 μg/mL Dox for 4 days. Expression of the different surface markers were analyzed by flow cytometry and compared to the expression by a parental hADMPCs. They were stained with PE-coupled antibodies against CD13, CD29, CD34, CD44, CD73, CD90, CD105, and CD166. Histogram of a PE-coupled mouse IgG1 κ isotype control is shown in gray. CMV; hADMPCs transduced with pTRE-EGFP-CMV-tTA-2A-Bsd, EF; hADMPCs transduced with pTRE-EGFP-EF-tTA-2A-Bsd.
doi:10.1371/journal.pone.0066274.g004

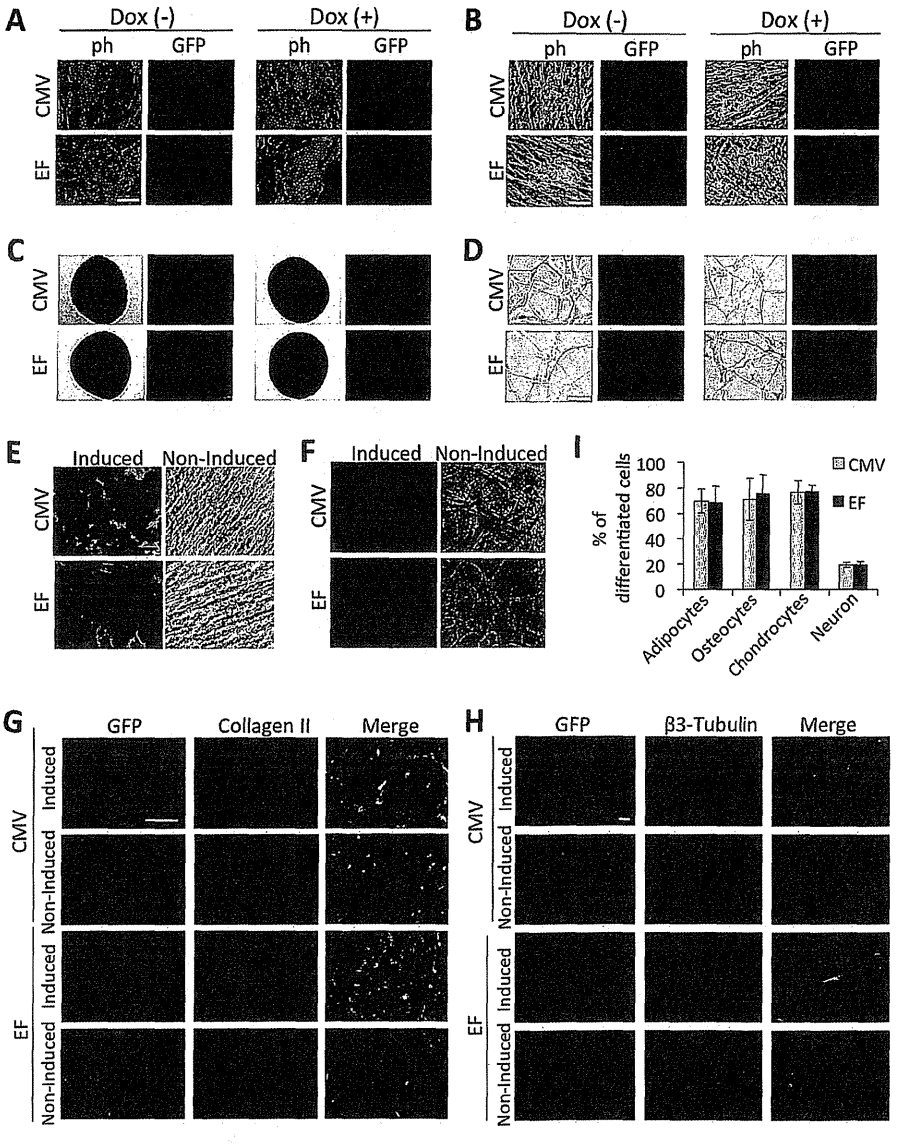

Figure 5. Differentiation potential of Dox-responsive hADMPCs. Dox-responsive hADMPCs were differentiated into adipocytes (A, E), osteocytes (B, F), chondrocytes (C, G), and neuronal cells (D, H). (A–D) Phase contrast (ph) and fluorescent (GFP) images. Dox-responsive hADMPCs were differentiated in the absence of Dox (Dox(−)) or in the presence of 1 μg/mL Dox (Dox(+)) as described in the material and methods section. (E–I) Confirmation of differentiated cells by oil red O staining for adipocytes (E), alizarin red staining for osteocytes (F), immunohistochemical staining against collagen II for chondrocytes (G), and immunohistochemical staining against β3-tubulin for neuronal cells (H). The percentages of differentiated cells to each cell type were calculated by the computerized image analysis (I). Cells that were not induced to differentiate (non-induced) were used as a negative control. CMV; hADMPCs transduced with pTRE-EGFP-CMV-tTA-2A-Bsd, EF; hADMPCs transduced with pTRE-EGFP-EF-tTA-2A-Bsd. Scale bar, 50 μm.
doi:10.1371/journal.pone.0066274.g005

requiring sustained, long-term expression of therapeutic proteins. In this study, we generated novel lentiviral vectors with a tet-off system, and demonstrated that our lentiviral vector systems were significantly effective and strictly regulated in hADMPCs, without affecting their stem cell properties.

Gene silencing is of considerable importance where stable, long-term expression is required. Researchers have reported that transgene silencing occurred when the CMV promoter was used in some cell types, especially in embryonic stem cells [15–17]. Since Kawabata et al. also demonstrated that virus-derived promoters inefficiently functioned in embryonic stem cells in gene transfer experiments [37], down-regulation and unsuitability of promoters in stem cells should be considered. Therefore, transduction efficacy and durability of transgene expression in hADMPCs is also an important issue to be determined. Qin et al. reported that the human EF-1α promoter and the TRE promoter are more efficient than the CMV promoter to drive lentiviral mediated transgene expression in rat bone marrow-derived MSCs [18]. McGinley et al. also showed that EF-1α and human phosphoglycerate kinase-1 (PGK) promoters have a clear advantage over the CMV promoter in transducing rat bone marrow-derived MSC transduction with lentivirus [19]. Consistent with their findings, our data also demonstrated that the EF-1α promoter was more efficient than the CMV promoter to drive EGFP expression in hADMPCs (Figure 1A, B). Moreover, a significant decrease in fluorescent intensity was observed by 28 days after transduction with lentiviral vector CSII-CMV-EGFP (Figure 1C), suggesting that the CMV promoter might be silenced in hADMPCs. We also demonstrated the intriguing finding that most (>90%) of the hADMPCs transduced with pTRE-EGFP-EF-tTA-2A-Bsd strongly expressed EGFP in the absence of Dox, whereas >50% of the cells transduced with pTRE-EGFP-CMV-tTA-2A-Bsd were EGFP negative, regardless of their blasticidin resistance (Figure 3A, B). Our data demonstrated that the inhibitor of histone deacetylation trichostatin A (TSA) re-induced the expression of EGFP (Figure 3C, D), suggesting that "promoter suppression" might occur by histone deacetylation, not by DNA methylation of CpG sites within the TRE tight promoter. "Promoter suppression" is a transcript repression of a 5′ transcriptional unit by a 3′ unit when 2 transcriptional units lie adjacent in head-to-tail tandem on a chromosome [28,29]. In this study, it is possible that the downstream unit of CMV-tTA-2A-Bsd repressed the upstream unit of TRE-EGFP because (1) resistance to blasticidin implies the transcriptional unit of CMV-tTA-2A-Bsd is active, and (2) reactivation of EGFP expression by TSA implies the transcriptional unit of TRE-EGFP is epigenetically silenced. In order to eliminate the promoter suppression or transcriptional interference between 2 transcriptional units, some researchers have been trying to separate the 2 units by polyadenylation, terminator, and insulator sequences [28,38]. However, these sequences extend the lentiviral vector size, which may affect the lentiviral titers produced from the vector. From this point of view, our finding that the transcriptional unit driven from the TRE tight promoter is resistant to gene silencing when arranged in tandem with the EF-tTA-2A-Bsd transcriptional unit (Figure 3) is of interest in the fields of both basic and clinical research, although the underlying mechanism remains elusive.

In general, large numbers of cells displaying the appropriate phenotypes are required for tissue engineering. Moreover, fully differentiated cells do not proliferate [39]. Therefore, in order to obtain enough cells to perform a transplant from genetically modified MSCs, it is important to develop a system in which the gene of interest is tightly regulated and inducible, and in which stably expressing transgenic cell lines can be obtained without affecting their stem cell properties. Using the system, MSCs transduced with lentiviral vectors can be selected and increased in numbers from a limited number of MSCs, before the target genes are induced. After obtaining an adequate number of gene-manipulated MSCs, the target genes could be induced in order to start differentiation. According to our data, hADMPCs transduced with pTRE-EGFP-EF-tTA-2A-Bsd were successfully selected by blasticidin, could proliferate, maintain their stem cell properties, and regulate EGFP expression tightly by Dox (Figure 4, 5), demonstrating that this all-in-one lentiviral vector is a promising gene delivery system for generating the material for artificial organs.

A major advantage of using the 2A cleavage factor in the construction of multi-cistronic vectors is its small size compared to internal promoter entry site (IRES) sequences. Because the titer of the lentivirus decreases with increasing size of the lentiviral vector, it is important to minimize the length of the sequences. In addition, linkage of 2 genes by 2A peptide resulted in efficient co-expression of the genes, whereas a gene placed downstream of an IRES is expressed at 2- to 3-fold lower levels than a gene placed upstream [40,41]. In this study, tTA-2A-Bsd cassette driven from CMV or EF-1α promoter showed ~90% cleavage (Figure 3). However, the point that should be considered is the effect of residual 2A peptide on the protein. As the processing occurred at the end of the 2A peptide, the 2A tag remains attached at the tTA C-terminus. Our data demonstrated that the presence of this extra 2A peptide did not seem to interfere with the activity of tTA since Dox strictly regulated the expression of EGFP under the control of TRE-tight promoter (Figure 2D, 3A, 3B and 5). Moreover, when Bsd is cleaved, an additional proline is attached at the N-terminus. We demonstrated that this did not affect a function of Bsd because hADMPCs transduced with either pTRE-EGFP-CMV-tTA-2A-Bsd or pTRE-EGFP-EF-tTA-2A-Bsd could survive and proliferate in medium containing blasticidin at a concentration at which all of the parental hADMPCs died.

Another advantage of our lentiviral system is the availability of a restriction enzyme treatment/ligation independent cloning system, called the Gateway system (Invitrogen). In general, the construction of lentiviral vectors using a conventional restriction enzyme/ligation cloning method has poor efficiency due to the large sizes and the lack of proper cloning sites. In our hands, cloning efficiency into our new lentiviral vectors pTRE-RfA-CMV-tTA-2A-Bsd or pTRE-RfA-EF-tTA-2A-Bsd using LR recombination reaches nearly 100%, saving time and effort in construction of the vectors. In addition, there are several resources available that take advantage of the Gateway vector. For example, CCSB Human ORFeome Collection (Dana-Farber Cancer Institute, Center for Cancer Systems Biology) represents almost 12,000 fully-sequenced cloned human ORFs which can be readily transferred to Gateway compatible destination vectors for various functional proteomics studies [42]. Block-iT pol II miR RNAi system from Invitrogen, which is designed to express artificial miRNAs, also enables compatibility with Gateway destination vectors for gene knock-down experiments [43].

In conclusion, our new single tet-off lentiviral vector system provides powerful tools not only for applied research on hADMPCs and other stem cells, but also basic research on a variety of cell lines and primary cells.

Acknowledgments

We thank J. Uda, S. Tamura, C. Sone, K. Nakagita, and H. Isshi for technical support. We thank Dr. Tyler Jacks for providing the pSico plasmid and Dr. Hiroyuki Miyoshi for the CSII-EF-RfA, CSII-CMV-RfA, pCMV-VSVG-RSV-Rev, and pCAG-HIVg/p plasmids.

Author Contributions

Conceived and designed the experiments: HM MM. Performed the experiments: HM MM KS HO AM. Analyzed the data: HM MM KS. Contributed reagents/materials/analysis tools: HM MM HO AI AM. Wrote the paper: HM MM TH.

References

1. Okura H, Komoda H, Saga A, Kakuta-Yamamoto A, Hamada Y, et al. (2010) Properties of hepatocyte-like cell clusters from human adipose tissue-derived mesenchymal stem cells. Tissue engineering Part C, Methods 16: 761–770.
2. Okura H, Matsuyama A, Lee CM, Saga A, Kakuta-Yamamoto A, et al. (2010) Cardiomyoblast-like cells differentiated from human adipose tissue-derived mesenchymal stem cells improve left ventricular dysfunction and survival in a rat myocardial infarction model. Tissue engineering Part C, Methods 16: 417–425.
3. Okura H, Komoda H, Fumimoto Y, Lee CM, Nishida T, et al. (2009) Transdifferentiation of human adipose tissue-derived stromal cells into insulin-producing clusters. Journal of artificial organs : the official journal of the Japanese Society for Artificial Organs 12: 123–130.
4. Safford KM, Safford SD, Gimble JM, Shetty AK, Rice HE (2004) Characterization of neuronal/glial differentiation of murine adipose-derived adult stromal cells. Experimental neurology 187: 319–328.
5. Leu S, Lin YC, Yuen CM, Yen CH, Kao YH, et al. (2010) Adipose-derived mesenchymal stem cells markedly attenuate brain infarct size and improve neurological function in rats. Journal of translational medicine 8: 63.
6. Ikegame Y, Yamashita K, Hayashi S, Mizuno H, Tawada M, et al. (2011) Comparison of mesenchymal stem cells from adipose tissue and bone marrow for ischemic stroke therapy. Cytotherapy 13: 675–685.
7. Tan B, Luan Z, Wei X, He Y, Wei G, et al. (2011) AMP-activated kinase mediates adipose stem cell-stimulated neuritogenesis of PC12 cells. Neuroscience 181: 40–47.
8. Reid AJ, Sun M, Wiberg M, Downes S, Terenghi G, et al. (2011) Nerve repair with adipose-derived stem cells protects dorsal root ganglia neurons from apoptosis. Neuroscience.
9. Rehman J, Traktuev D, Li J, Merfeld-Clauss S, Temm-Grove CJ, et al. (2004) Secretion of angiogenic and antiapoptotic factors by human adipose stromal cells. Circulation 109: 1292–1298.
10. Lee EY, Xia Y, Kim WS, Kim MH, Kim TH, et al. (2009) Hypoxia-enhanced wound-healing function of adipose-derived stem cells: increase in stem cell proliferation and up-regulation of VEGF and bFGF. Wound repair and regeneration : official publication of the Wound Healing Society [and] the European Tissue Repair Society 17: 540–547.
11. Moriyama M, Moriyama H, Ueda A, Nishibata Y, Okura H, et al. (2012) Human adipose tissue-derived multilineage progenitor cells exposed to oxidative stress induce neurite outgrowth in PC12 cells through p38 MAPK signaling. BMC Cell Biol 13: 21.
12. Wu H, Ye Z, Mahato RI (2011) Genetically modified mesenchymal stem cells for improved islet transplantation. Mol Pharm 8: 1458–1470.
13. Pfeifer A, Ikawa M, Dayn Y, Verma IM (2002) Transgenesis by lentiviral vectors: lack of gene silencing in mammalian embryonic stem cells and preimplantation embryos. Proc Natl Acad Sci U S A 99: 2140–2145.
14. Duan HF, Wu CT, Wu DL, Lu Y, Liu HJ, et al. (2003) Treatment of myocardial ischemia with bone marrow-derived mesenchymal stem cells overexpressing hepatocyte growth factor. Mol Ther 8: 467–474.
15. Brooks AR, Harkins RN, Wang P, Qian HS, Liu P, et al. (2004) Transcriptional silencing is associated with extensive methylation of the CMV promoter following adenoviral gene delivery to muscle. J Gene Med 6: 395–404.
16. Kim S, Kim GJ, Miyoshi H, Moon SH, Ahn SE, et al. (2007) Efficiency of the elongation factor-1alpha promoter in mammalian embryonic stem cells using lentiviral gene delivery systems. Stem Cells Dev 16: 537–545.
17. Meilinger D, Fellinger K, Bultmann S, Rothbauer U, Bonapace IM, et al. (2009) Np95 interacts with de novo DNA methyltransferases, Dnmt3a and Dnmt3b, and mediates epigenetic silencing of the viral CMV promoter in embryonic stem cells. EMBO Rep 10: 1259–1264.
18. Qin JY, Zhang L, Clift KL, Hulur I, Xiang AP, et al. (2010) Systematic comparison of constitutive promoters and the doxycycline-inducible promoter. PLoS One 5: e10611.
19. McGinley L, McMahon J, Strappe P, Barry F, Murphy M, et al. (2011) Lentiviral vector mediated modification of mesenchymal stem cells & enhanced survival in an in vitro model of ischaemia. Stem Cell Res Ther 2: 12.
20. Weber W, Fussenegger M (2006) Pharmacologic transgene control systems for gene therapy. J Gene Med 8: 535–556.
21. Shi Q, Tian X, Zhao Y, Luo H, Tian Y, et al. (2011) Anti-arthritic effects of FasL gene transferred intra-articularly by an inducible lentiviral vector containing improved tet-on system. Rheumatol Int.
22. Wiederschain D, Wee S, Chen L, Loo A, Yang G, et al. (2009) Single-vector inducible lentiviral RNAi system for oncology target validation. Cell Cycle 8: 498–504.
23. Hioki H, Kuramoto E, Konno M, Kameda H, Takahashi Y, et al. (2009) High-level transgene expression in neurons by lentivirus with Tet-Off system. Neurosci Res 63: 149–154.
24. Benabdellah K, Cobo M, Munoz P, Toscano MG, Martin F (2011) Development of an all-in-one lentiviral vector system based on the original TetR for the easy generation of Tet-ON cell lines. PLoS One 6: e23734.
25. Okura H, Saga A, Fumimoto Y, Soeda M, Moriyama M, et al. (2011) Transplantation of human adipose tissue-derived multilineage progenitor cells reduces serum cholesterol in hyperlipidemic Watanabe rabbits. Tissue engineering Part C, Methods 17: 145–154.
26. Saga A, Okura H, Soeda M, Tani J, Fumimoto Y, et al. (2011) HMG-CoA reductase inhibitor augments the serum total cholesterol-lowering effect of human adipose tissue-derived multilineage progenitor cells in hyperlipidemic homozygous Watanabe rabbits. Biochemical and biophysical research communications 412: 50–54.
27. Okura H, Saga A, Fumimoto Y, Soeda M, Moriyama M, et al. (2011) Transplantation of human adipose tissue-derived multilineage progenitor cells reduces serum cholesterol in hyperlipidemic Watanabe rabbits. Tissue Eng Part C Methods 17: 145–154.
28. Villemure JF, Savard N, Belmaaza A (2001) Promoter suppression in cultured mammalian cells can be blocked by the chicken beta-globin chromatin insulator 5'HS4 and matrix/scaffold attachment regions. J Mol Biol 312: 963–974.
29. Emerman M, Temin HM (1986) Comparison of promoter suppression in avian and murine retrovirus vectors. Nucleic Acids Res 14: 9381–9396.
30. Tai K, Pelled G, Sheyn D, Bershteyn A, Han L, et al. (2008) Nanobiomechanics of repair bone regenerated by genetically modified mesenchymal stem cells. Tissue Eng Part A 14: 1709–1720.
31. Goudenege S, Pisani DF, Wdziekonski B, Di Santo JP, Bagnis C, et al. (2009) Enhancement of myogenic and muscle repair capacities of human adipose-derived stem cells with forced expression of MyoD. Mol Ther 17: 1064–1072.
32. Li Y, Zhang R, Qiao H, Zhang H, Wang Y, et al. (2007) Generation of insulin-producing cells from PDX-1 gene-modified human mesenchymal stem cells. J Cell Physiol 211: 36–44.
33. Karnieli O, Izhar-Prato Y, Bulvik S, Efrat S (2007) Generation of insulin-producing cells from human bone marrow mesenchymal stem cells by genetic manipulation. Stem Cells 25: 2837–2844.
34. Dezawa M, Kanno H, Hoshino M, Cho H, Matsumoto N, et al. (2004) Specific induction of neuronal cells from bone marrow stromal cells and application for autologous transplantation. J Clin Invest 113: 1701–1710.
35. Fan L, Lin C, Zhuo S, Chen L, Liu N, et al. (2009) Transplantation with survivin-engineered mesenchymal stem cells results in better prognosis in a rat model of myocardial infarction. Eur J Heart Fail 11: 1023–1030.
36. Ghosh SS, Gopinath P, Ramesh A (2006) Adenoviral vectors: a promising tool for gene therapy. Appl Biochem Biotechnol 133: 9–29.
37. Kawabata K, Sakurai F, Yamaguchi T, Hayakawa T, Mizuguchi H (2005) Efficient gene transfer into mouse embryonic stem cells with adenovirus vectors. Mol Ther 12: 547–554.
38. Tian J, Andreadis ST (2009) Independent and high-level dual-gene expression in adult stem-progenitor cells from a single lentiviral vector. Gene Ther 16: 874–884.
39. Clarke MF, Fuller M (2006) Stem cells and cancer: two faces of eve. Cell 124: 1111–1115.
40. Chinnasamy D, Milsom MD, Shaffer J, Neuenfeldt J, Shaaban AF, et al. (2006) Multicistronic lentiviral vectors containing the FMDV 2A cleavage factor demonstrate robust expression of encoded genes at limiting MOI. Virol J 3: 14.
41. Ibrahimi A, Vande Velde G, Reumers V, Toelen J, Thiry I, et al. (2009) Highly efficient multicistronic lentiviral vectors with peptide 2A sequences. Hum Gene Ther 20: 845–860.
42. Temple G, Gerhard DS, Rasooly R, Feingold EA, Good PJ, et al. (2009) The completion of the Mammalian Gene Collection (MGC). Genome Res 19: 2324–2333.
43. Liang Z, Wu H, Reddy S, Zhu A, Wang S, et al. (2007) Blockade of invasion and metastasis of breast cancer cells via targeting CXCR4 with an artificial microRNA. Biochem Biophys Res Commun 363: 542–546.

Role of Notch signaling in the maintenance of human mesenchymal stem cells under hypoxic conditions

Hiroyuki Moriyama[1,*], Mariko Moriyama[1,*], Haruki Isshi[1], Shin Ishihara[1], Hanayuki Okura[2], Akihiro Ichinose[3], Toshiyuki Ozawa[4], Akifumi Matsuyama[2] and Takao Hayakawa[1]

[1] Pharmaceutical Research and Technology Institute, Kinki University, Higashi-Osaka, Osaka, Japan.

[2] Platform of therapeutics for Rare Disease and Health Policy, National Institute of Biomedical Innovation, Kobe, Hyogo, Japan.

[3] Department of Plastic Surgery, Kobe University Hospital, Kobe, Hyogo, Japan.

[4] Department of Dermatology, Osaka City University, Graduate School of Medicine, Osaka, Japan.

*These two authors contributed equally to this work.

Running title: MESENCHYMAL STEM CELLS UNDER HYPOXIA

Address correspondence to:

Dr. Hiroyuki Moriyama

Pharmaceutical Research and Technology Institute

Kinki University

3-4-1 Kowakae

Higashi-Osaka

Osaka 577-8502

Japan

Tel&Fax: +81-6-4307-4312

Email: moriyama@phar.kindai.ac.jp

Abstract

Human adipose tissue-derived multilineage progenitor cells (hADMPCs) are attractive for cell therapy and tissue engineering because of their multipotency and ease of isolation without serial ethical issues. However, their limited *in vitro* lifespan in culture systems hinders their therapeutic application. Some somatic stem cells including hADMPCs are known to be localized in hypoxic regions; thus, hypoxia may be beneficial for *ex vivo* culture of these stem cells. These cells exhibit a high level of glycolytic metabolism in presence of high oxygen levels and further increase their glycolysis rate under hypoxia. However, the physiological role of glycolytic activation and its regulatory mechanisms are still incompletely understood. Here we show that Notch signaling is required for glycolysis regulation under hypoxic conditions. Our results demonstrate that 5% O_2 dramatically increased the glycolysis rate, improved the proliferation efficiency, prevented senescence, and maintained the multipotency of hADMPCs. Intriguingly, these effects were not mediated by hypoxia-inducible factor (HIF), but rather by the Notch signaling pathway. 5% O_2 significantly increased the level of activated Notch1 and expression of its downstream gene, *HES1*. Furthermore, 5% O_2 markedly increased glucose consumption and lactate production of hADMPCs, which decreased back to normoxic levels upon treatment with a γ-secretase inhibitor. We also found that HES1 was involved in induction of GLUT3, TPI, and PGK1 in addition to reduction of TIGAR and SCO2 expression. These results clearly suggest that Notch signaling regulates glycolysis under hypoxic conditions and thus likely affects the cell lifespan via glycolysis.

Introduction

Human adipose tissue-derived mesenchymal stem cells (MSCs), also referred to as human adipose tissue–derived multilineage progenitor cells (hADMPCs), are multipotent stem cells that can differentiate into various types of cells, including hepatocytes [1], cardiomyoblasts [2], pancreatic cells [3], and neuronal cells [4-6]. They can be easily and safely obtained from lipoaspirate without posing serious ethical issues and can also be expanded *ex vivo* under appropriate culture conditions. Moreover, MSCs, including hADMPCs, have the ability to migrate to injured areas and secrete a wide variety of cytokines and growth factors necessary for tissue regeneration [7-11]. In addition, because of their hypoimmunogenicity and immunomodulatory effects, hADMPCs are good candidates as gene delivery vehicles for therapeutic purposes [12]. Thus, hADMPCs are attractive seeding cells for cell therapy and tissue engineering. However, similar to other somatic stem cells or primary cells, hADMPCs have limited growth potential and ultimately stop proliferation as a result of cellular senescence [13], which hinders their therapeutic application.

Conversely, embryonic stem cells (ESCs) and induced pluripotent stem cells (iPSCs) are immortal under standard culture conditions. Recently, several groups have reported that these cells greatly rely on glycolysis for energy production even under high-oxygen conditions [14-16]. This phenomenon is known as the Warburg effect and was originally described for cancer cells by Otto Warburg in the 1920s [17]. Although mitochondrial respiration is more efficient than glycolysis in generating ATP (net yield of 30 ATPs vs. 2 ATPs), glycolysis is able to produce ATP considerably faster than mitochondrial respiration as long as glucose supplies are adequate. Thus,

a metabolic shift from mitochondrial respiration to glycolysis would provide a growth advantage for actively proliferating cells. Moreover, Kondoh *et al.* demonstrated that enhanced glycolysis is also involved in cellular immortalization through reduction of intrinsic ROS production [14,18,19]. Because accumulation of intrinsic ROS levels could be a major reason for replicative senescence [20], enhancing glycolysis in cultured cells might improve the quality of the cells by suppressing premature senescence. One candidate method for induction of glycolysis is application of low-oxygen conditions to activate the transcription factor, hypoxia-inducible factor (HIF). HIF-1 is known to increase the expression of most glycolytic enzymes and the glucose transporters GLUT1 and GLUT3 [20]. Thus, several studies have reported that hypoxia is beneficial for the maintenance of hESCs in a pluripotent state [21,22]. Moreover, low oxygen tension has been reported to enhance the generation of induced pluripotent stem cells both from mouse and human primary fibroblasts [23].

Recently, hypoxic culture conditions have also been reported to confer a growth advantage, prevent premature senescence, and maintain undifferentiated states in somatic stem cells, e.g., hematopoietic stem cells (HSCs) [24], neural stem cells [25], and bone marrow-derived MSCs [26]. These stem cells reside in their local microenvironments called the "stem cell niche", where the oxygen tension is relatively low (in the range of 1%–9%). Thus, hypoxic culture may be beneficial to these stem cells with regard to in vitro proliferation, cell survival, and differentiation. Takubo et al. reported that HSCs activated Pdk through HIF1α in hypoxic culture conditions, resulting in maintenance of glycolytic flow and suppression of the influx of glycolytic metabolites into mitochondria, and this glycolytic metabolic state was shown to be indispensable for the maintenance of HSCs [27]. Several studies have reported that MSCs exhibit a high level of glycolytic metabolism in the presence of high oxygen

levels and further increase their rate of glycolysis upon culture under hypoxia [28,29]. However, a relationship between beneficial effects of hypoxic conditions and metabolic status in addition to involvement of HIFs in the metabolic changes has not been investigated in these reports.

In this study, we aimed to investigate the effect of 5% oxygen on hADMPCs. Our results demonstrate that culture under 5% oxygen increased the glycolysis rate, improved the proliferation efficiency, prevented the cellular senescence, and maintained the undifferentiated status of hADMPCs. Intriguingly, these effects were not mediated by HIF, but rather by Notch signaling, an important signaling pathway required for the development of many cell types and maintenance of stem cells [30,31]. 5% oxygen activated Notch signaling, resulting the upregulation of *SLC2A3*, *TPI*, and *PGK1* in addition to the downregulation of *TIGAR* and *SCO2*, which may contribute to the increase in the glycolysis rate. These observations thus provide new regulatory mechanisms for stemness maintenance obtained under 5% oxygen conditions.

Material and Methods

Adipose tissue samples

Subcutaneous adipose tissue samples (10–50 g each) were resected during plastic surgery from 5 female and 2 male patients (age 20–60 years) as discarded tissue. The study protocol was approved by the Review Board for Human Research of Kobe University Graduate School of Medicine Foundation for Biomedical Research and

Innovation, Osaka City University Graduate School of Medicine, and Kinki University Pharmaceutical Research and Technology Institute (reference number: 12-043). Each subject provided signed informed consent.

Cell culture

hADMPCs were isolated as previously reported [32-35] and maintained in a medium containing 60% DMEM-low glucose, 40% MCDB-201 medium (Sigma Aldrich, St. Louis, MO, USA), 1× insulin-transferrin-selenium (Life Technologies, NY, USA), 1 nM dexamethasone (Sigma Aldrich), 100 mM ascorbic acid 2-phosphate (Wako, Osaka, Japan), 10 ng/mL epidermal growth factor (PeproTech, NJ, USA), and 5% fetal bovine serum. The cells were plated to a density of 5×10^3 cells/cm^2 on fibronectin-coated dishes, and the medium was replaced every 2 days. For hypoxic culture, cells were cultured in a gas mixture composed of 90% N_2, 5% CO_2, and 5% O_2. For maintenance of the hypoxic gas mixture, a ProOx C21 carbon dioxide and oxygen controller and a C-Chamber (Biospherix, NY, USA) were used.

Senescence-associated β-galactosidase staining

Cells were fixed with 2% paraformaldehyde/0.2% glutaradehyde for 5 min at room temperature and then washed 2 times with phosphate-buffered saline (PBS). The cells were then incubated overnight at 37 °C with fresh senescence-associated β-galactosidase (SA-β-Gal) chromogenic substrate solution (1 mg/mL Bluo-gal (Life

Technologies), 40 mM citric acid (pH 6.0), 5 mM potassium ferrocyanide, 5 mM potassium ferricyanide, 150 mM NaCl, and 2 mM $MgCl_2$).

Measurement of reactive oxygen species production

Cells were harvested and incubated with 10 μM 5-(and-6)-chloromethyl-2',7'-dichlorodihydrofluorescein diacetate, acetyl ester (CM-H_2DCFDA). The amount of intracellular ROS production was proportional to the green fluorescence, as analyzed using a Guava EasyCyte 8HT flow cytometer (Millipore, MA, USA) using an argon laser at 488 nm and a 525/30 nm band pass filter, and dead cells were excluded using the Live/Dead Fixable Far Red Dead Cell Stain Kit (Life Technologies).

EdU proliferation assay

For assessment of cell proliferation, hADMPCs were seeded on a fibronectin-coated 6-well plate at a density of 5 × 10^3 cells/cm^2 and cultured for 3 days. Cell proliferation was detected by incorporating of 5-ethynyl-2'-deoxyuridine (EdU) and using the Click-iT EdU Alexa Fluor 488 Flow Cytometry Assay Kit (Life Technologies). Briefly, according to the manufacturer's protocol, cells were incubated with 10 μM EdU for 2 h before fixation, permeabilized, and stained with EdU. EdU-positive cells were then analyzed using the 488 nm laser of a Guava EasyCyte 8HT flow cytometer (Millipore).

Flow cytometry analysis

Flow cytometry analysis was performed as previously described [35]. Briefly, hADMPCs were harvested and re-suspended in staining buffer (PBS containing 1% BSA, 2 mM EDTA, and 0.01% sodium azide) at a density of $1x10^6$ cells/mL, incubated for 20 min with a fluorescein isothiocyanate (FITC)-conjugated antibody against CD49b or CD98 (BioLegend, CA, USA) or a phycoerythrin (PE)-conjugated antibody against CD10, CD13, CD29, CD44, CD49a, CD49c, CD49d, CD49e, CD51/61, CD73, CD90, CD105, CD117, SSEA4, HLA-A,B,C (BioLegend), CD133/1 (Miltenyi Biotec, CA, USA), or CD166 (Beckman Coulter, CA, USA). Non-specific staining was assessed using relevant isotype controls. Dead cells were excluded using the Live/Dead Fixable Far Red Dead Cell Stain Kit (Life Technologies). FlowJo software was used for quantitative analysis.

RNA extraction, cDNA generation, and quantitative polymerase chain reaction (Q-PCR)

Total RNA was extracted using the RNeasy Mini Kit (Qiagen, Hilden, Germany) accroding to the manufacturer's instructions. cDNA was generated from 1 µg of total RNA using the Verso cDNA Synthesis Kit (Thermo Scientific, MA, USA) and purified using the MinElute PCR Purification Kit (Qiagen). Q-PCR analysis was conducted using the SsoFast EvaGreen supermix (Bio-Rad, CA, USA) according to the manufacturer's protocols. The relative expression value for each gene was calculated using the ΔΔCt method and the most reliable internal control gene

was determined using geNorm Software (http://medgen.ugent.be/~jvdesomp/genorm/). Details of the primers used in these experiments are available upon request.

Western blot analysis

Whole cell extracts were prepared by washing cells with ice-cold phosphate-buffered saline (PBS) and lysing them with M-PER Mammalian Protein Extraction Reagent (Thermo Scientific Pierce, IL, USA) according to the manufacturer' s instructions. Nuclear and cytosolic extracts were prepared as follows. Cells were washed with ice-cold PBS and lysed with lysis buffer (50 mM Tris-HCl (pH 7.5), 0.5% Triton X-100, 137.5 mM NaCl, 10% glycerol, 5 mM EDTA, 1 mM sodium vanadate, 50 mM sodium fluoride, 10 mM sodium pyrophosphate, and protease inhibitor cocktail). Then, insoluble nuclei were isolated by centrifugation and lysed with lysis buffer containing 0.5% SDS. Equal amounts of proteins were separated by sodium dodecyl sulfate polyacrylamide gel electrophoresis (SDS-PAGE), transferred to polyvinylidene fluoride (PVDF) membranes (Immobilon-P; Millipore), and probed with antibodies against cleaved Notch1 (#2421, Cell Signaling Technology, MA, USA), HIF-1α (#610959, BD Bioscience, CA, USA), hypoxia inducible factor 2α (MAB3472, Millipore), Akt (#9272, Cell Signaling Technology), and phospho Akt (Ser473) (#4060, Cell Signaling Technology). Horseradish peroxidase (HRP)-conjugated anti-mouse or -rabbit IgG antibody (Cell Signaling Technology) was used as a secondary antibody and immunoreactive bands were visualized using Immobilon Western Chemiluminescent HRP substrate (Millipore). The band intensity was measured using the ImageJ software.

Fluorescence microscopy

Phase contrast and fluorescence images were obtained using a fluorescence microscope (BZ-9000; Keyence, Osaka, Japan) using BZ Analyzer Software (Keyence).

Adipogenic, osteogenic, and chondrogenic differentiation procedures

For adipogenic differentiation, cells were cultured in differentiation medium (Zen-Bio, NC, USA). After 7 days, half of the medium was exchanged for adipocyte medium (Zen-Bio) and this was repeated every 3 days. Three weeks after differentiation, adipogenic differentiation was confirmed by microscopic observation of intracellular lipid droplets with the aid of Oil Red O staining. Osteogenic differentiation was induced by culturing the cells in osteocyte differentiation medium (Zen-Bio). Differentiation was examined by Alizarin Red staining. For chondrogenic differentiation, 2×10^5 hADMSCs were centrifuged at 400 × *g* for 10 min. The resulting pellets were cultured in chondrogenic medium (Lonza, Basel, Switzerland) for 21 days. The pellets were fixed with 4% paraformaldehyde in PBS, embedded in OCT, frozen, and sectioned at 8 μm. The sections were incubated with PBSMT (PBS containing 0.1% Triton X-100, and 2% skim milk) for 1 h at room temperature, and then incubated with a mouse monoclonal antibody against type II collagen (Abcam, MA, USA) for 1 h. After washing with PBS, cells were incubated with Alexa 546-conjugated anti-mouse IgG to identify chondrocytes (Life Technologies). The

cells were counterstained with 4'-6-diamidino-2-phenylindole (DAPI) (Life Technologies) to identify cellular nuclei. The sections were also stained with 1% alcian blue (Sigma Aldrich) in 3% acetic acid, pH 2.5 for 30 min.

Determination of HK, PFK, LDH, PDH, and Cox IV activities

Cells (2×10^6) were lysed, and HK, PFK, LDH, or PDH activity was measured using the Hexokinase Colorimetric Activity Kit, Phosphofructokinase (PFK) Activity Colorimetric Assay Kit, Lactate Dehydrogenase (LDH) Activity Assay Kit, or Pyruvate Dehydrogenase Activity Colorimetric Assay Kit (all from BioVision, Milpitas, CA, USA) respectively, according to the manufacturer's instructions. To measure Cox IV activity, mitochondria were isolated from 2×10^7 cells using a Mitochondria Isolation Kit (Thermo Scientific) and lysed with buffer containing n-Dodecyl β-D-maltoside, followed by measurement with the Mitochondria Activity Assay (Cytochrome C Oxidase Activity Assay) Kit (BioChain Institute, Newark, CA, USA), according to the manufacturer's instructions.

Results

5% Oxygen hypoxic culture condition increases proliferation capacity and decreases senescence

hADMPCs were cultured under 20% oxygen (normoxia; Nx) or 5% oxygen (hypoxia; Hx) and their proliferation capacities were examined based on the relationship between the number of cultivation days and the population

doubling level (PDL). Nx-cultured hADMPCs ceased proliferation at a PDL of 35–40 (between 46–70 days), whereas continuous cell proliferation beyond 45 PDL was observed when hADMPCs were cultured in the Hx condition (Figure 1A). To investigate whether this increase of PDL in the Hx culture condition resulted from an increase in cell cycle progression and increase in survival rates, 5-ethynyl-2'-deoxyuridine (EdU), an alternative to 5-bromo-2'-deoxyuridine (BrdU), was incorporated into the genomic DNA of the hADMPCs, and the amount of incorporated EdU was quantified by flow cytometry. As shown in Figure 1B, the EdU incorporation rate was significantly higher in Hx-cultured hADMPCs than in Nx-cultured hADMPCs, suggesting that cell growth was increased in the Hx culture condition. In addition, measurement of DNA content in hADMPCs revealed a slight but significant decrease of sub-G1 peaks, which indicates the existence of apoptotic cells with degraded DNA, when the cells were cultured in the Hx condition (Figure 1C). These data suggest that the Hx culture condition increases the proliferation capacity of hADMPCs by promoting their cell growth and survival rates. We also found that Nx-cultured hADMPCs were larger with a more irregular shape (Figure 1D), which suggests that the Hx culture condition prevented hADMPCs from entering senescence [36]. To further investigate this phenomenon, cellular senescence was measured by staining for senescence-associated β-galactosidase (SA-β-Gal), which revealed that SA-β-Gal activity was increased in Nx-cultured hADMPCs at passage 17 (Figure 1E). As it has been hypothesized that senescence results from oxidative stress [20], accumulation of reactive oxygen species (ROS) in hADMPCs was detected using the non-fluorescent probe, CM-H_2DCFDA. Flow cytometry analysis revealed that ROS were generated at higher levels in hADMPCs when cultured in the Nx condition (Figure 1F), suggesting that reduced production of ROS in the Hx condition may prevent the cells from entering replicative senescence.

Hypoxic culture maintains some mesenchymal stem cell properties and increases differentiation

We then examined the cell properties of hADMPCs under Nx and Hx conditions. Initially, cell surface antigens expressed on hADMPCs were analyzed by flow cytometry. No significant difference in expression profile between hADMPCs cultured in Nx and Hx was observed; the cells were consistently positive for CD10, CD13, CD29, CD44, CD49a, CD49b, CD49c, CD49d, CD49e, CD51/61, CD54, CD59, CD73, CD90, CD98, CD105, CD166, and HLA-A, B, C, but negative for CD34, CD45, CD117, CD133 (Figure 2 and data not shown). These data were consistent with previous reports describing the expression profiles of cell surface markers of hMSCs [37,38]. To further examine the stem cell properties of hADMPCs, their potential for differentiation into adipocyte, osteocyte, and chondrocyte lineages was analyzed at passage 8. Hx-cultured hADMPCs presented enhanced differentiation into various lineages (Figure 3A and B), indicating that the Hx culture condition improved the stem cell properties of hADMPCs.

Hypoxic culture condition activates Notch signaling

To reveal the molecular mechanism by which the Hx culture condition increased the proliferative capacity and maintaining the stem cell properties of hADMPCs, we next examined Notch signaling, which is required for maintaining stem-cell features of various types of stem cells [30,31]. As expected, levels of cleaved NOTCH1, an

activated form of NOTCH1, were significantly increased (> 2-fold) in the Hx culture condition (Figure 4A). Quantitative PCR (Q-PCR) analysis revealed that HES1, a downstream target of Notch signaling, was upregulated in Hx-cultured hADMPCs, which also indicated that Notch signaling was activated in the Hx culture condition (Figure 4B). Administration of the γ-secretase inhibitor DAPT at 1 μM, which was sufficient to inhibit the proteolytic cleavage of NOTCH1 (Figure 4A), decreased the Hx-induced expression of HES1 at both mRNA and protein levels (Figure 4B and C). These data indicate that Hx increased the expression of HES1 through activation of Notch signaling. It has been reported that Notch signaling and hypoxia-inducible factor (HIF) undergo cross talk in hypoxic cells [39-42]. Therefore, HIF-1α and HIF-2α protein levels in hADMPCs were analyzed by western blotting. HIF-1α was stabilized when a chemical hypoxia-mimicking agent, cobalt chloride, was applied in the culture, whereas no obvious increase of HIF-1α was observed in the Hx culture condition (Figure 4D). However, we did not detect any HIF-2α expression even in the presence of cobalt chloride (Figure 4E). Q-PCR analysis revealed that *HIF2A* mRNA was not expressed in these cells (data not shown). From these results, we concluded that neither HIF-1α nor HIF-2α was involved in the Hx-induced increase in the proliferative capacity and stem cell properties of hADMPCs.

To identify the signaling responsible for the observed effect, we next examined the Akt, NF-κB, and p53 signaling pathways. It has been reported that hypoxic conditions induce the activation of Akt and NF-κB signaling [43,44]. In addition, hypoxic conditions have been shown to inhibit p53 activity [45], and crosstalk between these pathways and Notch signaling has also been demonstrated [42,46-48]. As shown in Figure 4F, the

Hx condition increased Akt phosphorylation, which was not decreased by DAPT treatment. These data demonstrate that 5% oxygen activated Akt signaling but not via Notch signaling. Similarly, the hypoxic condition induced nuclear accumulation of p65, which was inhibited by DAPT treatment (Figure 4G). These data suggest that NF-κB signaling is regulated by Notch signaling in hADMPCs. Furthermore, p53 was not activated under the 5% oxygen condition as assessed by detection of phospho-p53 and a p53 reporter assay. However, DAPT treatment significantly increased p53 activity (Figure 4H and I).

Notch signaling is indispensable for acquisition of the advantageous properties of hADMPCs

We next examined the roles of Notch signaling in the proliferative capacity and stem cell properties of hADMPCs in the Hx culture condition. To inhibit Notch signaling, DAPT was added to the medium at a final concentration of 1 μM. DAPT treatment significantly decreased the PDL when hADMPCs were cultured under either 20% or 5% oxygen (Figure 5A). Intriguingly, measurement of the DNA content in hADMPCs revealed that inhibition of Notch signaling by 1 μM DAPT significantly attenuated the decrease in apoptotic cells in the Hx condition (Figure 5B). These data suggest that 5% oxygen increases the proliferation capacity of hADMPCs through Notch signaling by promoting their survival. To examine whether Notch signaling affects the stem cell properties of hADMPCs, differentiation into adipocyte, osteocyte, and chondrocyte lineages was analyzed at passage 8. Hx-cultured hADMPCs underwent greater differentiated into all lineages as described in Figure 3, whereas application of a Notch inhibitor significantly decreased the differentiation capacity to all lineages (Figure 5C-E). In addition,

SA-β-Gal staining revealed that inhibition of Notch signaling by DAPT remarkably promoted senescence in both the Nx and Hx culture conditions, suggesting that the suppression of replicative senescence observed in the Hx condition is mediated by Notch signaling.

Glycolysis is enhanced in the 5% oxygen condition through Notch signaling

Recent studies suggest that the metabolic shift from aerobic mitochondrial respiration to glycolysis extends the life span possibly via reduction of intrinsic ROS production [18,19]. Our results demonstrate that the 5% oxygen condition reduced ROS accumulation in hADMPCs (Figure 1F). In addition, the relationship between Notch signaling and glycolysis has been recently established [49,50]. We therefore considered glycolytic flux by measuring the glucose consumption and lactate production of hADMPCs in the Nx or Hx culture conditions. As shown in Figure 6A, glucose consumption and lactate production were elevated in the Hx culture condition, indicating that a metabolic shift to glycolysis occurred when hADMPCs were cultured in 5% oxygen. In contrast, the Notch inhibitor DAPT markedly reduced glycolytic flux as assessed by glucose consumption and lactate production (Figure 6A). To identify the genes responsible for the glycolytic change, we performed a Q-PCR analysis. As shown in Figure 6B, *SLC2A3, TPI, and PGK1*, encoding glycolytic enzymes, were upregulated in the 5% oxygen condition, whereas these genes were suppressed by DAPT treatment. Interestingly, Hes1 transduction by an adenoviral vector markedly induced the mRNA expression of the same genes (Figure 6E). In addition, SCO2, a positive modulator of aerobic respiration, and TIGAR, a negative regulator of glycolysis, were

transcriptionally downregulated in the 5% oxygen condition, whereas DAPT treatment partially restored the expression level (Figure 6B). Adenoviral expression of Hes1 dramatically reduced *SCO2* and *TIGAR* expression (Figure 6E), which suggests that the Notch-Hes1 signaling modulates the metabolic pathway. We also measured the activities of key enzymes in glycolysis. Hexokinase activity was not changed under hypoxic conditions; however, phosphofructokinase and lactate dehydrogenase were activated in 5% oxygen condition, which was attenuated by Notch inhibition (Figure 6C). In addition, pyruvate dehydrogenase (PDH) and cytochrome c oxidase (Complex IV) activity assays showed that mitochondrial respiration decreased under the hypoxic condition and that DAPT treatment restored it (Figure 6D). Moreover, glycolytic flux in Hes1-expressing hADMPCs was positively correlated with the expression of these glycolytic genes as assessed by glucose consumption and lactate production (Figure 6F). In contrast, HES1 knockdown by adenoviral transduction of *HES1* RNAi resulted in a significant reduction of glycolytic flux (Figure 6G), demonstrating that HES1 is involved in the regulation of glycolysis.

Glycolysis supports the proliferation of hADMPCs

To determine whether aerobic glycolysis is important for the proliferation of hADMPCs, hADMPCs were treated with the glycolytic inhibitor 2-deoxy-D-glucose (2-DG) or the respiration inhibitor sodium azide (NaN_3). We found that hADMPCs were sensitive to treatment with 2-DG even at the low concentration of 0.2 mM (Figure 7A). In contrast, treatment of hADMPCs with NaN_3, rather increased their proliferation at the concentration of 1 mM and